EFDA–JET–CP(08)03-21

L. Lauro-Taroni, G. Corrigan, A. Foster, M.O'Mullane, V. Parail, J. Strachan,
H.P. Summers, A. Whiteford, S. Wiesen and JET EFDA contributors

Assessment of the Superstage Description of Heavy Impurities for JET and ITER

Assessment of the Superstage Description of Heavy Impurities for JET and ITER

L. Lauro-Taroni[1], G. Corrigan[2], A. Foster[3], M. O'Mullane[3], V. Parail[2], J. Strachan[4], H.P. Summers[3], A. Whiteford[3], S. Wiesen[5] and JET EFDA contributors*

JET-EFDA, Culham Science Centre, OX14 3DB, Abingdon, UK

[1]Consorzio RFX, ENEA Euratom Association, Padova, Italy
[2]EURATOM-UKAEA Fusion Association, Culham Science Centre, OX14 3DB, Abingdon, OXON, UK
[3]Strathclyde University, Glasgow, U.K.
[4]PPPL, Princeton University, Princeton NJ, 08543 USA
[5]IPP-IEF, Forschungszentrum Jülich GmbH, Euratom Association, TEC,D-52425 Jülich, Germany
** See annex of M.L. Watkins et al, "Overview of JET Results ",*
(Proc. 21 st IAEA Fusion Energy Conference, Chengdu, China (2006)).

Preprint of Paper to be submitted for publication in Proceedings of the
35th EPS Conference on Plasma Physics, Hersonissos, Crete, Greece
(9th June 2008 - 13th June 2008)

INTRODUCTION

Reliable simulations of the transport of heavy impurities in JET are necessary for the prediction of ITER performance. The standard treatment in impurity transport codes is to solve the fluid equations for all Z ionic stages of an impurity (all-ion model). In the case of Tungsten, this means solving 74 equations. In the superstage treatment [1, 2] the number of working populations is reduced to less than Z with each such population consisting of a 'bundle' of contiguous ionisation stages'– called a 'superstage'. The base model of the superstage description is that the ions bundled in each superstage are constrained to be in coronal equilibrium between each other. From the numerical point of view, the treatment of a heavy impurity in superstages cuts down the number of equations and, more importantly, makes the numerical techniques used in 2-D edge codes more stable when the densities are very low. The bundling scheme ('partition') is made to reflect the natural spatio-temporal clustering of ionisation stages in the plasma.

In this paper we present the first results of the validation and comparison of some different bundling schemes for Ni and W against the all-ion model and against each other.

The JET EFDA jams suite of codes has been upgraded to enable the 1.5-D core impurity transport code SANCO (coupled with the energy transport code JETTO) and the 2-D SOL/edge fluid code EDGE2D/EIRENE [3,4] to model impurities bundled into superstages. In the case of the SANCO, heavy impurities can be simulated both in the all-ion stage model as well as bundled in any user-devised partition: so it is possible to gain experience and compare the various partitions between each other and with the full-ion model.

Both for SANCO and EDGE2D, the choice of superstage partition must be done beforehand and the necessary ADAS datasets for ionisation, recombination and the calculation of the radiated power must be prepared from the all-ion datasets. The number of equations to be solved in the transport codes is cut down, but each superstage *k* has a charge and ionisation potential which varies with the local T_e (and n_e). Where T_e is lower the superstage charge is weighed towards the lower Z ions in its bundle. The so-called 'natural bundling' follows the shell's structure by bundling ions whose ionisation potential is close. For Ni the number of populations is cut from 28 down to 12 and for W from 74 to 35. Other bundling schemes are possible, depending on the plasma conditions (e.g. on Te) or on available CPU time, with more aggressive partitions of W into 26 and even 9 superstages being reported here.

1-D NI SIMULATIONS

A transient influx of Ni in a JET plasma has been used to assess the Ni natural bundling: Figures 1a and 1b show the Te and ne profiles. The Ni anomalous diffusion and convection are the same for all Ni populations (Fig.1c). The all-ion and the naturally bundled (12 superstages) simulations are compared in Fig.2, where the total Ni content (2a) and the volume integrated Ni radiation (2b) are shown for the two cases. Figure 2c shown the radiation due to the Non-Equilibrium (NE) electron cooling term arising from the departure from coronal equilibrium of the populations,$\propto \Sigma\,(I_{Z+1} S_Z n_Z - I_Z R_{Z+1} n_{Z+1})$, where S_Z represents the ionisation from Z→Z+1 and R_{Z+1} is the recombination from Z+1→Z and Ik is the ionisation potential of stage *k*. This term in the core plasma is usually negligible, but it can be noticed that it is significant (about 20%) during the ingress phase. This can

be interpreted as a consequence of the departure from coronal equilibrium and could be used as an indicator of the goodness of the bundling scheme employed.

1-D W SIMULATIONS

The above set-up is repeated, substituting Ni with W. Figure 3 shows the time histories of the full 74-ion W, compared with bundling into 35, 26 and 9 superstages. In the 9-superstage picture, all the ions with an ionisation potential >1keV have been bundled together. The agreement is remarkably good, indicating that for the transport in fig1c at least the W radiation can be reasonably estimated from the coronal approximation.

W has been simulated for a peaked ITER scenario 4 (Fig.4) assuming a fully neoclassical convection v calculated with NCLASS during the simulation and keeping the W content constant in time to highlight the effect of transport in the redistribution of W. Because of ∇n_e (Fig.4a) and T_e (Fig.4b) close to the separatrix, the neoclassical velocity of W at the edge is directed outwards, while in the core it is mildly inwards (Fig.4d). In these simulations, the initial W profile (Fig.4c, solid line) evolves in a fixed background plasma: the W profiles are shown after 10sec for the various cases (74, 35, 26 and 9 superstages) and they are barely distinguishable. The CPU consumption for the SANCO part of the neoclassical simulation is cut by a factor ~7-8 between the 74 ions and the 9 superstages cases. All the different partitions capture the essential feature of this plasma configuration: the outwards v at the edge screens the W penetration: in these conditions the core peaking of W is benign. It is important to stress that a small difference in the edge ne would alter the resulting neoclassical v and reverse its sign from outwards to inwards: in this case central peaking of W leads to an unsustainable accumulation.

2-D W SIMULATIONS

The extrapolation of the above results on W bundling to the SOL/edge plasmas is non-trivial: for edge 2-D codes it is unfeasible to simulate all 74 W ions and only different partitions can be compared with each other. There are also issues specific to the SOL region which are not present in the core simulations. As an example of 2-D simulations, a trace amount of W enters from the wall a JET plasma with C as the main light impurity. Fig 5 shows the W density along the separatrix and along the outer target. For comparison, the C density is of order $10^{17}\,m^{-3}$. The two sets of curves are from two different simulations, both with W bundled into 9 superstages, but with different groupings of the ions: the bundling of the red curve is more aggressive on the lower ions than the black curve.

CONCLUSIONS

The JET EFDA suite of codes jams has now the capability of simulating Tungsten. A few examples of simulations of W in the core and in the edge have been shown. The superstages' description has been compared with the standard all-ion description for the core transport: it captures the essential physics, while reducing the computational effort. The bundling in superstages makes edge simulations of W possible. First examples have been shown and a systematic exploration of the migration of W due to effects which are important for C, and of the impact of different bundling schemes on it, is now possible.

ACKNOWLEDGEMENT:

This work was carried out within the framework of the EFDA. The views and opinions expressed herein do not necessarily reflect those of the European Commission.

REFERENCES

[1]. H.P. Summers et al. 5th ICAMDATA, Vol901, pag239-248,

[2]. X.Bonnin et al: EPS 2007,

[3]. R.Simonini et al, CPP 34, p368(1994),

[4]. D.Reiter et al, http://www.eirene.de

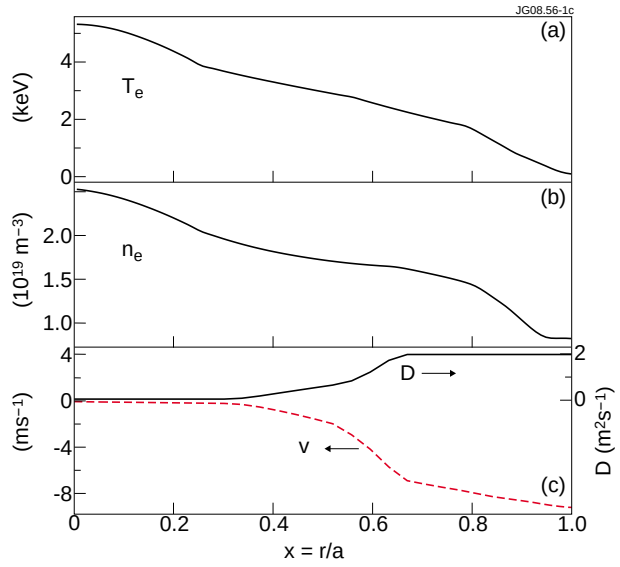

Figure 1:

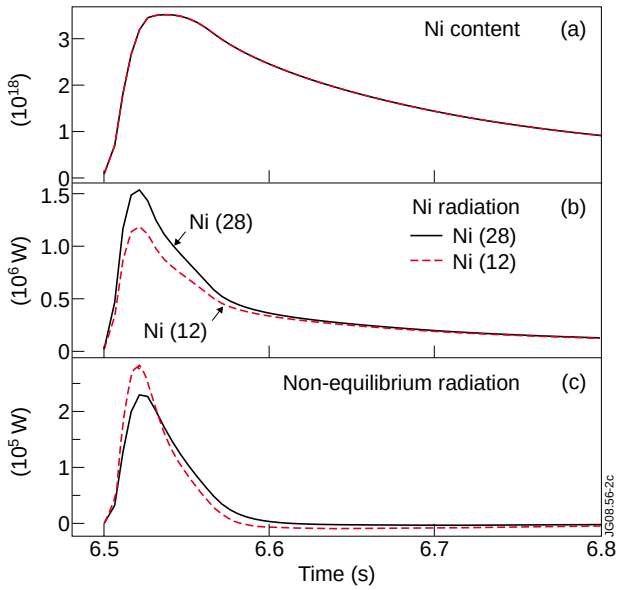

Figure 2:

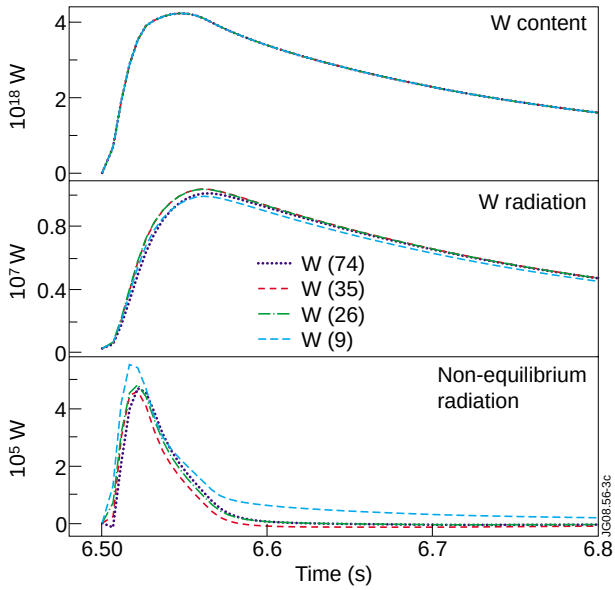

Figure 3:

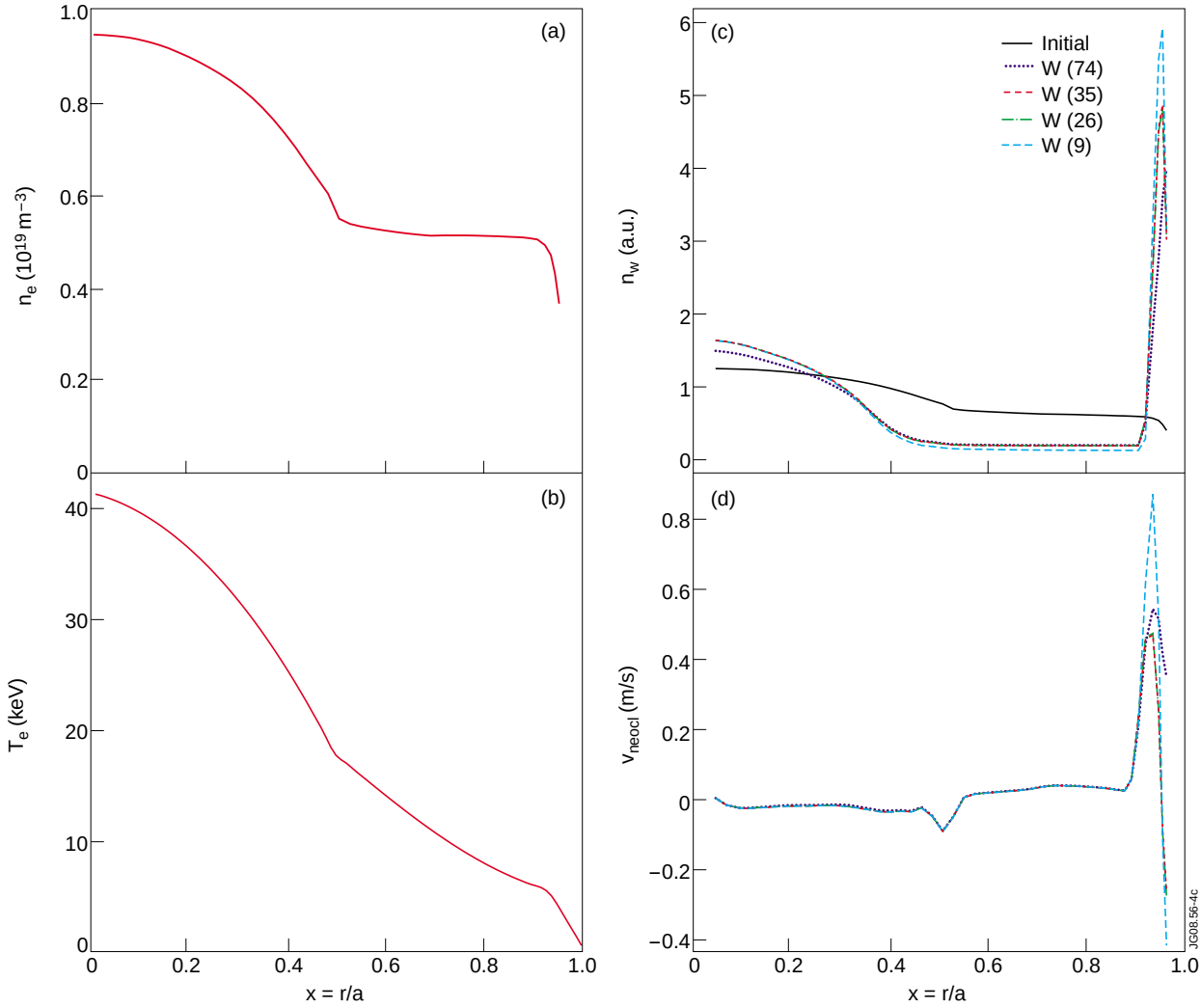

Figure 4:

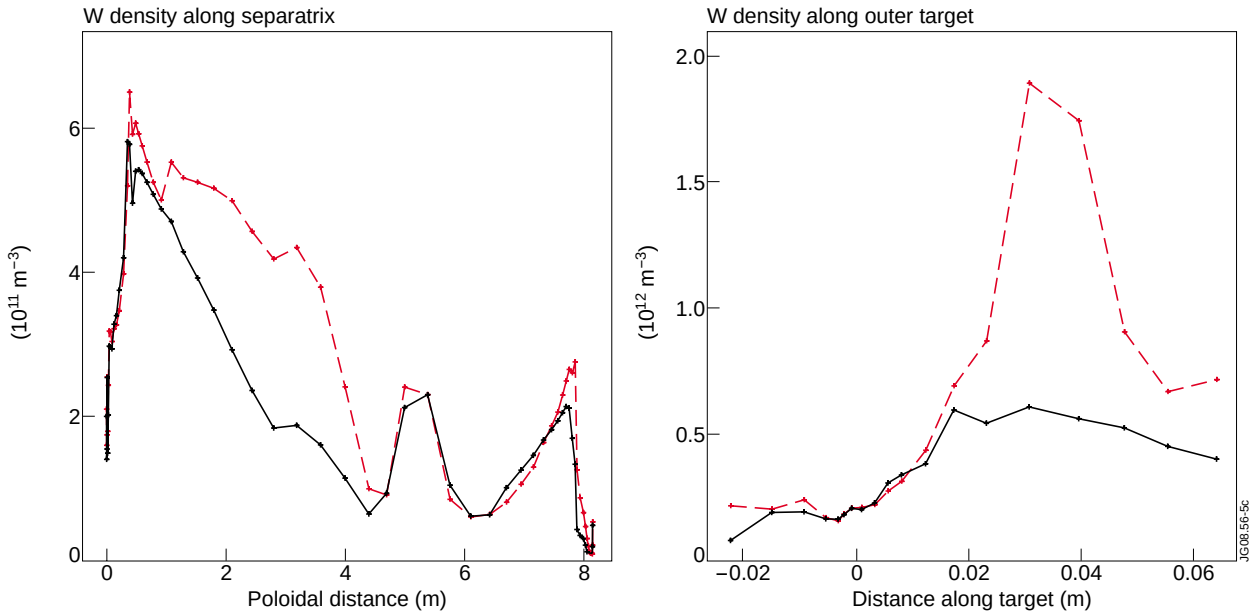

Figure 5: